RESEARCH ARTICLE

Research on Adaptive ORB-SURF Image Matching Algorithm Based on Fusion of Edge Features

LENG HAN[1], JIAWEI WANG[1], YI ZHANG[1], XIA SUN[2], AND XUHUI WU[1]
[1]School of Advanced Manufacturing Engineering, Chongqing University of Posts and Telecommunications, Chongqing 400065, China
[2]Chongqing Institute of Engineering, Chongqing 400056, China

Corresponding author: Xia Sun (sunxia@cqie.edu.cn)

ABSTRACT The traditional speeded-up robust features (SURF) algorithm has certain stability in scale, rotation, illumination and other changes. However, this algorithm has problems such as large amount of computation, low matching accuracy, and time-consuming in feature extraction and feature matching. An improved adaptive ORB-SURF image matching algorithm is proposed in this paper. Fusing edge features and using improved Oriented FAST and Rotated BRIEF (ORB) algorithms are used by this algorithm to extract image feature points. Moreover, SURF descriptors are used by feature points for feature description. Then an improved fast library for approximate nearest neighbors (FLANN) algorithm was used for adaptive feature matching. The random sample consensus (RANSAC) algorithm is used to eliminate the false matching point pairs after the selected points to be matched. Finally, the excellent matching point pairs reserved by the adaptive FLANN algorithm are combined with the excellent matching point pairs reserved by the RANSAC algorithm to complete the matching. The experimental results show that the average accuracy of the improved algorithm can reach more than 98%, which is about 6% higher than the original SURF algorithm. And the average matching time is 1.2S, which is about 25% lower than the original SURF algorithm. It is worth mentioning that the problem that the original SURF algorithm cannot predict the number of feature points through Hessian threshold is solved by this algorithm. Moreover, compared with the SuperPoint based deep learning image matching algorithm, the image matching time of this algorithm is reduced by 80%.

INDEX TERMS SURF algorithm, edge detection, image matching, ORB algorithm, FLANN algorithm, RANSAC algorithm.

I. INTRODUCTION

With the development of science and technology, computer vision technology has been gradually applied in many fields such as mobile robot V-SLAM, medical [1] and video image stitching [2]. A large number of computer vision problems around image registration have been proposed at this stage [3], [4], [5], [6]. The detection and matching of feature points are regarded as the basis for realizing image matching, image fusion and 3D imaging.

In the image registration algorithm, establishing the registration relationship between images with image feature points is considered as the main method. The concept of feature points and the corner detection algorithm were proposed by Moravec [7], but this algorithm cannot achieve image registration after image rotation and scale changes. Subsequently, The image scale space was proposed and constructed by Harris [8], Lindeberg [9], etc. First, the corner features were constructed by calculating the eigenvalues of 2×2 matrices containing image information, and then Gaussian convolution was performed. This method enables the images to have better matching effects at different scales. The scale invariant feature transform (SIFT) algorithm was

The associate editor coordinating the review of this manuscript and approving it for publication was Gustavo Olague.

proposed by DavidG. Lowe [10], which has strong robustness and scale invariance. However, due to its 128-dimensional feature description vector, it consumes a lot of time in data processing. The SURF algorithm based on the SIFT algorithm was proposed by Bay [11]. The feature vector of this algorithm was reduced in dimension, which shortened the matching time, but the matching accuracy was reduced. Song Jiaqian et al. [12] used the edge detection method to improve the feature extraction operator, and used the gradient feature of the image to describe the feature. However, the feature matching of the algorithm only relies on the Euclidean distance measurement method, which leads to a decrease in the matching accuracy. Chen Wei et al. [13] replaced SURF blobs with FAST corner points to extract feature points, and then used SURF descriptor to describe the feature points. The traditional SURF algorithm has a long computational time problem solved by this method, but the matching accuracy is very low in terms of scale invariance.

Aiming at the problems of long image matching time and low accuracy, an improved SURF feature matching algorithm that fuses edge features and ORB feature points extraction is proposed in this paper. Two aspects of feature point detection and adaptive threshold matching are improved by this algorithm. Firstly, edge feature detection is carried out, and the improved ORB algorithm is used to extract image edge feature points. Firstly, the edge features of the image are detected, and the improved ORB algorithm is used to extract the edge feature points of the image. This not only limits the number of feature point detections, but also reduces the matching time and avoids the influence of factors such as lighting on the matching. The SURF descriptor is then used by the algorithm for feature point description. The improved adaptive FLANN algorithm was then used for image matching. Finally, combined with the RANSAC algorithm, the false matching point pairs are further removed to complete the matching.

II. ALGORITHM FLOW

The flow chart of the algorithm in this paper is shown in Fig.1.

The traditional SURF algorithm has problems such as requiring a preset threshold to extract feature points, and the number of feature points is unpredictable, resulting in long matching time and low matching accuracy. Edge feature detection and ORB algorithm are studied and further improved in this paper. Edge feature detection eliminates the influence of image noise and illumination on feature point detection. When the improved ORB algorithm is used to extract image edge feature points, the method can determine the optimal top n feature points by the preset number of feature points. Then, during feature extraction, the scale space is established and the direction information of the feature point is added, so that the feature point has scale invariance and specific direction information.

The nearest neighbor algorithm has the problems that the preset threshold cannot achieve the best matching effect, and the method takes a long time and has low accuracy.
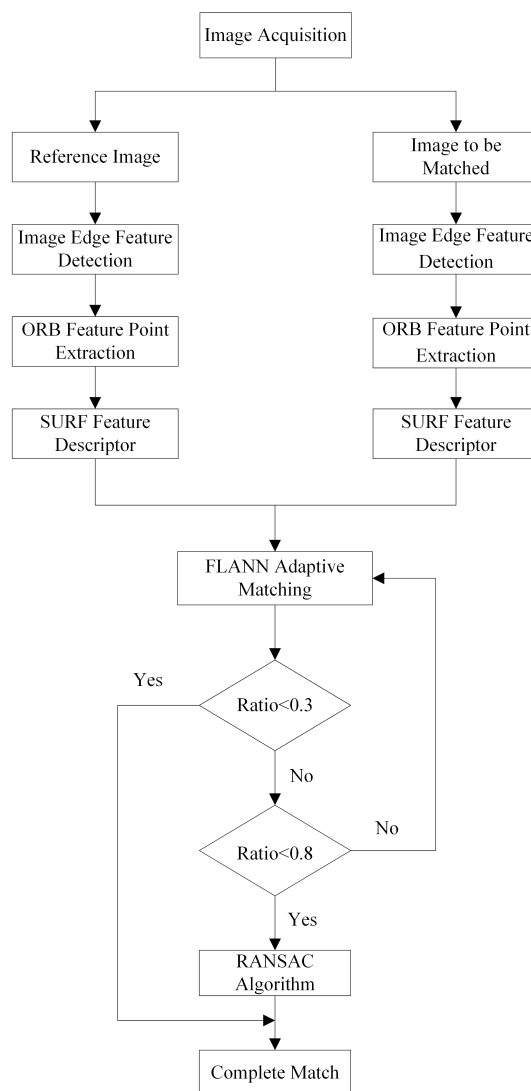

FIGURE 1. The algorithm flow of this paper.

The adaptability of the nearest neighbor algorithm is proposed in this paper, which can further improve the accuracy of the algorithm and reduce the matching time. Specifically, through the control of a specific threshold, the feature point pairs are selected and divided into excellent matching point pairs, to-be-matched point pairs and poor matching point pairs. Then, the matching feature point pairs to be matched are screened and combined with the excellent matching point pairs.

III. EDGE DETECTION

In edge detection, pixels whose gray value changes drastically in the image are formed into a pixel set. Then, the feature structure of the original image is determined through the pixel set. Finally, the edge features of the image are obtained from the feature structure.

In edge detection algorithms, Sobel operator, Canny operator and Log operator are more common [14]. This paper
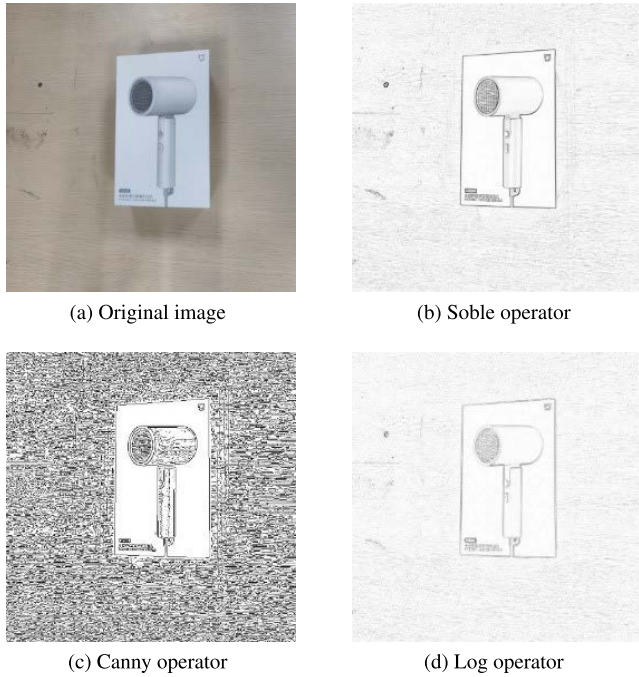
(a) Original image

(b) Soble operator

(c) Canny operator

(d) Log operator

FIGURE 2. The effect of different operators for edge detection.

$$G_x$$

$$G_y$$

FIGURE 3. Sobel operator horizontal and vertical gradient template.

compares the edge feature detection experiments by applying Soble operator, Canny operator and Log operator to the hair dryer image. It can be seen from the experimental results that compared with the other two methods, the Sobel operator has achieved a better effect on the image edge retention, and the image edge texture is clear. Moreover, it also has a good denoising effect against the influence of the environment in the image, which is beneficial to the extraction of subsequent feature points. Fig. 2 shows the effect of edge feature detection.

The Sobel operator [15] uses the gray-scale weighted difference between upper and lower, left and right neighbors of the pixel to detect the edge, and the algorithm can provide edge direction information. The Sobel operator contains two 3×3 matrices, the horizontal matrix and vertical matrix. And using it to convolve with the image, the approximation of the horizontal and vertical matrices luminance difference can be obtained. A 3×3 area in the image is randomly selected as shown in the figure, and the horizontal and vertical gradient templates of the Sobel operator are shown in Fig. 3.

A represents the original image, G_x and G_y represent the gray value of the image after horizontal and vertical edge detection, respectively. Its formula is as follows:

$$G_x = \begin{bmatrix} -1 & 0 & +1 \\ -2 & 0 & +2 \\ -1 & 0 & +1 \end{bmatrix} * A \tag{1}$$

$$G_y = \begin{bmatrix} +1 & +2 & +1 \\ 0 & 0 & 0 \\ -1 & -2 & -1 \end{bmatrix} * A \tag{2}$$

$$A = \begin{bmatrix} f(x-1,y-1) & f(x-1,y) & f(x-1,y+1) \\ f(x,y-1) & f(x,y) & f(x,y+1) \\ f(x+1,y-1) & f(x+1,y) & f(x+1,y+1) \end{bmatrix} \tag{3}$$

According to the above gradient template, it is calculated by convolution with the pixels of the image. The formula is as follows:

$$G_x = [f(x+1,y-1) + 2*f(x+1,y) + f(x+1,y+1)] \\ - [f(x-1,y-1) + 2*f(x-1,y) + f(x-1,y+1)] \tag{4}$$

$$G_y = [f(x-1,y-1) + 2*f(x,y-1) + f(x+1,y-1)] \\ - [f(x-1,y+1) + 2*f(x,y+1) + f(x+1,y+1)] \tag{5}$$

Among them, $f(x, y)$ represents the gray value of (x, y) points in the image. The horizontal and vertical grayscale values of any pixel of the image are combined by the following formula to calculate the grayscale size of the point.

$$G(x, y) = \sqrt{G_x^2 + G_y^2} \approx |G_x| + |G_y| \tag{6}$$

An approximation of the pixel gradient can be obtained according to the above formula(6). By selecting an appropriate threshold and comparing the gradient approximation, if it is greater than the threshold, the point is an edge point, otherwise the point is not an edge point of the image [16], [17], [18], [19].

IV. FUSION IMPROVED ORB ALGORITHM

The ORB (Oriented FAST and Rotated BRIEF) algorithm [20] includes two parts, the FAST (feature from accelerated segment test) feature point detection method and the BRIEF (binary robust independent elementary feature) feature descriptor. The improved algorithm on the basis of the original mainly uses the gray centroid method to add direction information to the corner points extracted by FAST. This method provides rotation invariance for subsequent feature descriptions.

The FAST feature point extraction algorithm proposed by Edward Rosten [21] has the characteristics of fast calculation speed and good real-time performance. The definition of a feature point in the FAST algorithm is that if the gray value of a pixel is much larger or smaller than a certain range and a certain number of pixel gray values, the point may become a feature point. As shown in Fig. 4.
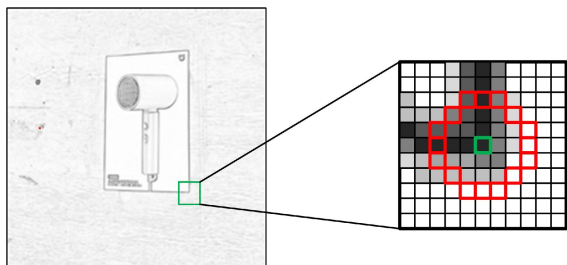
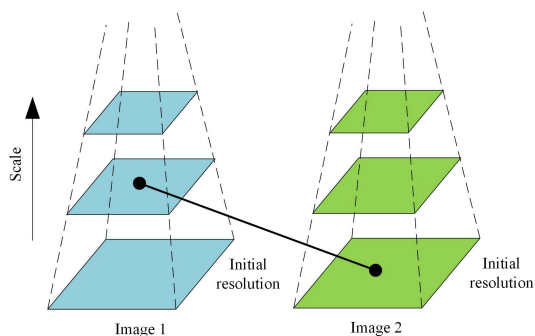**FIGURE 4.** Feature point detection template for the FAST algorithm.

FIGURE 5. Feature point detection template for the FAST algorithm.

TABLE 1. SURF algorithm flow.

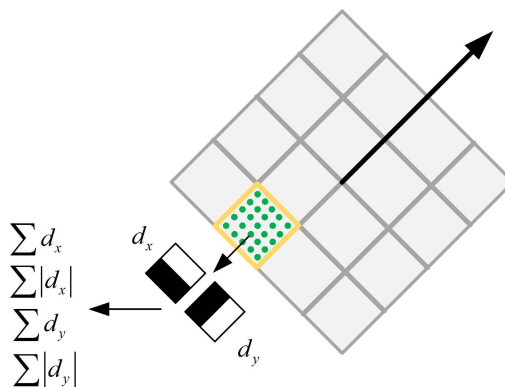| Algorithm Step	SURF
1	Image Input
2	Construct the Hessian Matrix
3	Build Scale Space
4	Preliminary Determination of Feature Points
5	Determine Feature Point Orientation
6	form Feature Point Descriptors

FIGURE 6. Descriptor representation.

The steps of detecting the to-be-detected point as a feature point are as follows.

Step 1: Count the gray value of point $P(x, y)$ to be detected as I_P.

Step 2: Take the point P to be detected as the center of the circle, take the distance of three pixels as the radius, and present a discretized circle with sixteen pixels on the circumference. As shown in Fig. 4.

Step 3: Specify a threshold value τ, and compare the point P to be detected with the sixteen feature points on the circumference. If the pixel gray value of N consecutive points is larger than $I_P + \tau$ or smaller than $I_P - \tau$. Then the point is determined as a feature point.

On the basis of the original algorithm, the concept of image pyramid is introduced into the improved ORB algorithm [22]. Specifically, when the feature point is judged, it is added and compared with the adjacent scale images, and the image pyramid is established to realize the scale invariance of the algorithm. As shown in Fig. 5.

The initial image is filtered first, and the Gaussian convolution of any given pixel $I(x, y)$ in the image at scale σ is shown below:

$$L(x, y, \sigma) = G(x, y\sigma) * I(x, y) \quad (7)$$

Among them, $L_{xy}(x, y, \sigma)$ is the result of convolution of Gaussian second-order partial derivative $\frac{\partial^2 g(\sigma)}{\partial x \partial y}$ with pixels. The Gaussian kernel function is:

$$G(\sigma) = \frac{1}{2\pi\sigma^2} e^{-(x^2+y^2)/2\sigma^2} \quad (8)$$

Starting from the lowest image, n images with different resolutions are finally generated, and the pixels of the images decrease in turn in the process of arranging upwards, and finally the topmost layer of the pyramid has only a single pixel. Feature points are extracted on each layer of the pyramid to achieve image matching at different scales or different resolutions.

V. SURF ALGORITHM

The SURF algorithm is a fast and robust local feature detection algorithm. Compared with the SIFT algorithm, the speed of the SURF algorithm is significantly improved. Integral images, box filters and dimensionality-reduced feature descriptors are introduced into the algorithm to achieve fast feature extraction. The main steps of the SURF algorithm are shown in Table 1.

The SURF descriptor builds a square neighborhood centered on the feature point with side lengths of 20S, where S refers to the scale. The algorithm not only has scale invariance, but also has rotation invariance. Specifically, the direction of the feature points is consistent with the direction of the square neighborhood, as shown in Fig. 6.

The algorithm samples in a square neighborhood at equal sampling intervals. The entire square area is divided into 16 sub-areas, each sub-area has 25 sampling pixels, and the whole area has a total of 400 sampling pixels.Then, the wavelet responses d_x and d_y in the sub-region are calculated, and the wavelet response values in the region are accumulated.Finally calculate the sum of absolute values. In this way, a 4-dimensional feature vector v can be obtained:

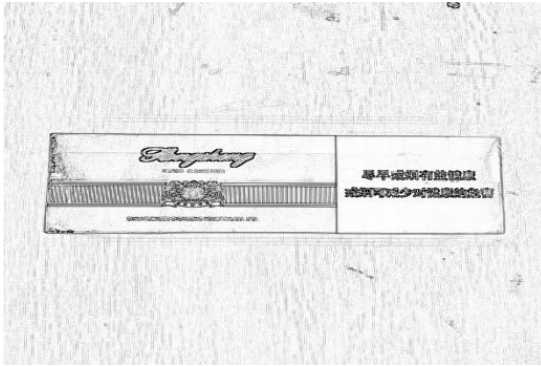$$\mathbf{v} = [\Sigma dx, \Sigma dy, \Sigma|dx|, \Sigma|dy|] \quad (9)$$

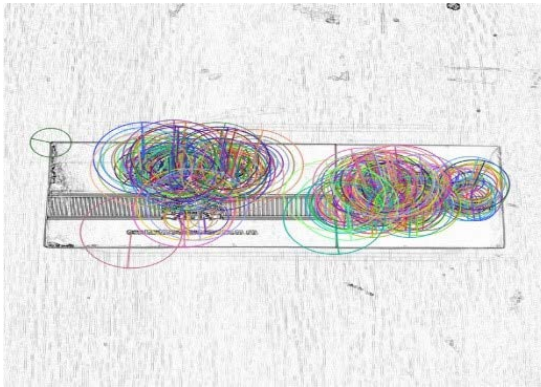**FIGURE 7.** Feature point detection template for the FAST algorithm.

FIGURE 8. Feature point detection template for the FAST algorithm.

The feature vectors v of the 16 sub-regions in the square field are combined, and finally such a 64-dimensional feature vector is normalized.

Assuming the SURF descriptor $P = \{p1, p2, \ldots, p64\}$ of the 64-dimensional feature vector, the normalization formula is:

$$q_i = \frac{p_i}{\sqrt{\sum_{j=1}^{64} p_j^2}}, \quad i = 1, 2, \ldots, 64 \tag{10}$$

Among them, $Q = \{q1, q2, \ldots, q64\}$ is the normalized feature vector.

As shown in the figure, Fig. 7 is the edge feature of the original image, and Fig. 8 is the direction and scale of the feature point after the edge feature is extracted by the ORB algorithm and described by the SURF algorithm.

VI. IMPROVED FLANN ADAPTIVE IMAGE MATCHING METHOD

The empirical threshold is used by the traditional FLANN algorithm to judge whether the matching point pairs match, which makes it very time-consuming to select a reasonable threshold on images of different complexity, and the matching accuracy cannot be guaranteed. This paper studies its self-adaptation, so that it can be well applied in different scenarios without preset threshold.

The FLANN algorithm [23], [24] performs preliminary matching on feature points by calculating the Euclidean distance between feature point descriptors to determine the matching degree of feature points. The algorithm generally selects two feature points closest to the feature point for calculation. First, take a feature point a in the feature point set A of the reference image, and find two feature points m and n with the closest Euclidean distance to point a in the feature point set B of the image to be matched. Finally, the nearest Euclidean distance and the second nearest Euclidean distance are obtained as D_{am} and D_{an}. The Euclidean distance expression is:

$$D(A, B) = \sqrt{\sum_{i=1}^{64} (v_{Ai} - u_{Bi})^2} \tag{11}$$

Among them, $D(A, B)$ is the Euclidean distance between points A and B, and A and B are the feature points of the reference image and the matching image point set, respectively. v_{Ai} and u_{Bi} represent the values of the i-th dimension of the feature descriptors of feature points A and B.

The traditional FLANN algorithm needs to preset a threshold value of τ. When the ratio of the nearest neighbor distance from the feature point to the point to be matched and the ratio of the feature point to the next nearest neighbor distance is less than the threshold, the matching is successful, and if it is greater than the threshold, the matching fails [25]. As shown in the following formula:

$$D_m/D_n < \tau \tag{12}$$

The FLANN algorithm needs a preset threshold to be improved in this paper. The improved method is to use the matching accuracy of different thresholds combined with the RANSAC algorithm to effectively remove the false matching to further optimize the matching accuracy and matching time-consuming problems. The preset threshold will not only cause the loss of a large number of feature matching point pairs to affect the matching accuracy, but also cause a lot of time-consuming preparatory work due to the need to select a reasonable threshold. By matching the image set, it is found that when the threshold is less than 0.3, the matching accuracy rate is over 99%. However, there are few feature point pairs at this time, and matching pairs can be retained at this time. When the threshold value is greater than 0.8, the false matching rate of the algorithm increases significantly, and there are more feature point pairs. Therefore, the utilization rate of the matching pair is low, and it is directly discarded. When the threshold value is between 0.3 and 0.8, the matching pairs are retained, and the RANSAC algorithm is used to eliminate false matching pairs. Finally, the excellent matching point pair set less than the threshold of 0.3 is combined with the feature point pair set that has eliminated the wrong matching point pair to complete the matching.
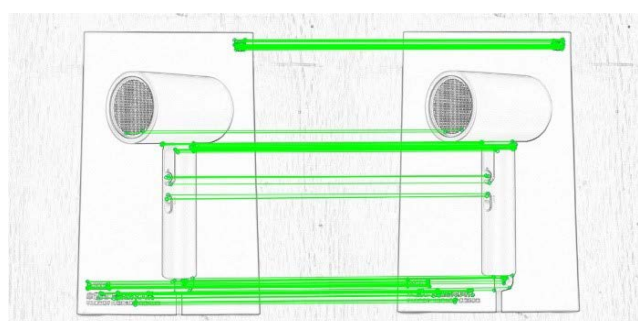
Table 2 shows the number of feature point pairs and matching accuracy of the FLANN matching algorithm obtained by taking different thresholds. It can be found that with
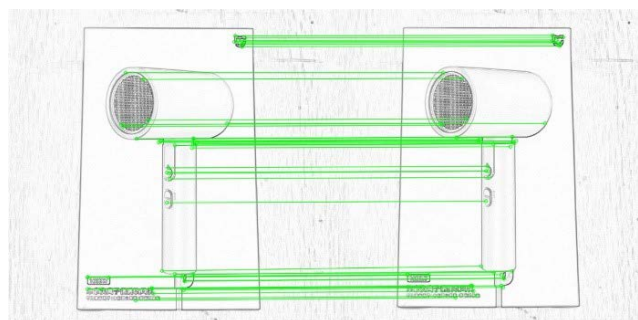
(a) Matching results with a threshold less than 0.3
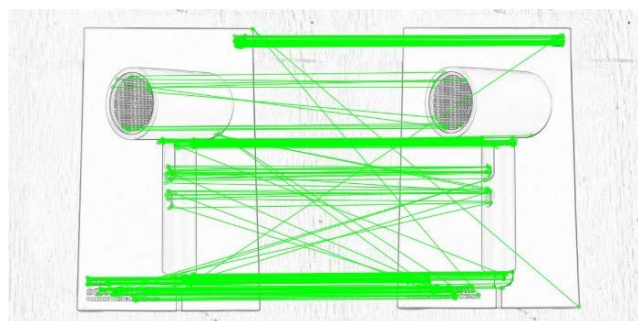
(b) Matching results with a threshold greater than 0.3 and less than 0.8

(c) Matching point pairs with a threshold between 0.3 and 0.8 after screening out the wrong matching pairs

FIGURE 9. Threshold matching experiment.

the increase of the threshold, the matching accuracy rate decreases continuously. When the threshold is less than 0.3, there are fewer matching point pairs, and the average matching accuracy is 99.42%. When the threshold is 0.8, the number of matching point pairs increases sharply, and the matching accuracy plummets to 70.63%.

Fig. 9(a) shows the matching results with a threshold less than 0.3. There are few matching point pairs, and the matching accuracy rate of the matching point pairs is high.Fig. 9(b) shows the matching results with a threshold greater than 0.3 and less than 0.8. There are many matching point pairs, and the number of incorrect matching point pairs increases significantly, and the matching accuracy rate is low.Fig. 9(c) shows the result of the matching point pairs with a threshold between 0.3 and 0.8 after further eliminating the wrong matching point pairs. The results show that a large number of incorrect matching point pairs are eliminated, and the matching accuracy of feature point pairs is significantly improved.

The improved algorithm achieves adaptability without preset thresholds.

VII. EXPERIMENTAL RESULTS AND ANALYSIS
The computer used in this experiment is HP Desktop Pro PCI MT, and its configuration is: CPU is i5-7500 processor, main frequency is 3.4GHz, and memory is 8G. The experiment adopts the SURF algorithm, the SuperPoint algorithm [26] and the ORB-SURF algorithm proposed in this paper to carry out matching control experiments, and the experimental data are the average of twenty experiments. This experiment mainly uses hair dryer boxes, mobile phone boxes and cigarette boxes as target objects. In the analysis of experimental results, the matching time is the sum of the time from the start of feature detection to the completion of matching. The accuracy measurement is based on the result of dividing the correct matching points by the total matching points.

A. EXPERIMENTAL ANALYSIS OF IMAGE MATCHING UNDER STABLE CONDITIONS
Fig. 10 is an image matching experiment on the picture set of hair dryer box. SURF algorithm is used by RANSAC algorithm and FLANN algorithm to extract image feature points. The deep learning method is used to extract image feature points by the SuperPoint algorithm. ORB algorithm is used by ORB-SURF matching to extract image feature points. Among them, the number of matching points obtained by the FLANN matching algorithm is as few as 48 pairs. There are many mismatches and invalid matching pairs outside the target object. After the RANSAC algorithm screening, the matching point pairs decreased to 38 pairs, and the false matching pairs and invalid matching pairs were also screened out to a certain extent. Based on the SuperPoint matching algorithm, 168 pairs of matching points are obtained in the image. After edge feature extraction, the adaptive ORB-SURF algorithm fused with ORB algorithm is adopted, and the matching point pairs are 131 pairs.

Table 3 is the average response time and accuracy information of each algorithm under the parallel viewing angle obtained in the experimental environment. Compared with the matching time of FLANN and RANSAC algorithm, the matching time of ORB-SURF algorithm is reduced by about 25%. Compared with the SuperPoint algorithm, the matching time of ORB-SURF algorithm is reduced by about 80%. In terms of matching accuracy, the matching accuracy of SuperPoint algorithm is 98.90%. The matching accuracy of ORB-SURF matching algorithm is 98.73%. The matching accuracy of RANSAC algorithm is 97.29%. The matching accuracy of FLANN algorithm is 92.13%. Compared with FLANN algorithm and RANSAC algorithm, ORB-SURF algorithm has significantly improved the matching accuracy and matching time. It is worth mentioning that compared with the SuperPoint algorithm, the matching time of this algorithm is reduced by about 80%, but the matching accuracy is only reduced by 0.17%.

TABLE 2. Effect of different thresholds on the accuracy of FLANN algorithm.

Threshold /τ	0.10	0.15	0.20	0.25	0.30	0.35	0.40	0.45	0.50
Feature Point Pairs	7	11	23	31	48	67	89	107	136
Matching Accuracy /%	99.92	99.81	99.78	99.69	99.42	98.92	98.50	96.72	94.37
Threshold /τ	0.55	0.60	0.65	0.70	0.75	0.80	0.85	0.90	0.95
Feature Point Pairs	156	182	193	217	231	285	347	403	486
Matching Accuracy /%	94.12	92.50	91.72	89.92	88.17	70.63	68.82	65.63	62.23

(a) FLANN matching

(b) RANSAC matching
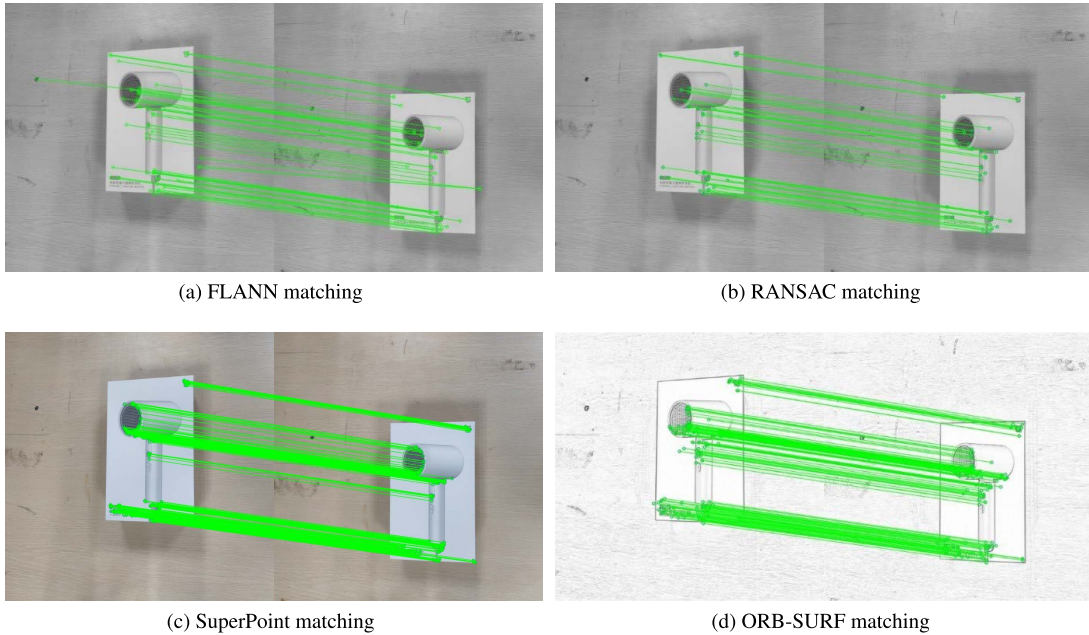
(c) SuperPoint matching

(d) ORB-SURF matching

FIGURE 10. Match experiment.

TABLE 3. Algorithm performance comparison in parallel.

Type	Average Response Time /s	Average Accuracy /%
FLANN	1.734	92.13
FLANN+RANSAC	1.750	97.29
SuperPoint	6.742	98.90
ORB-SURF	1.296	98.73

B. EXPERIMENTAL ANALYSIS OF IMAGE MATCHING UNDER COMPLEX CONDITIONS

In order to verify the reliability of the matching algorithm in the complex background, the algorithm performance was verified under the conditions of illumination transformation, scale transformation, and rotation transformation. Fig. 11 shows the matching in different lighting environments. Fig. 11(a), Fig. 11(b) and Fig. 11(c) are the matching results in a weak light environment, while Fig. 11(d), Fig. 11(e) and Fig. 11(f) are the matching results in a strong light environment. It can be found that under weak lighting environments, FLANN matching produces obvious mismatches. Among them, the accuracy rate is 96.70% in strong light environment and 92.10% in low light environment. It can be seen that with the enhancement of the light intensity to a certain extent, the matching accuracy of the

FLANN algorithm continues to rise. The matching accuracy of the SuperPoint algorithm remains above 99% in the case of changing illumination, but the matching time is long. The ORB-SURF algorithm has no obvious mismatch under the two lighting conditions. The average matching accuracy of this algorithm is about 99%, and the matching time is only one fifth of that of SuperPoint algorithm.

Fig. 12 shows the matching results when the image is scaled and rotation transformed. As shown in Fig. 12(a), Fig. 12(b) and Fig. 12(c), FLANN algorithm, SuperPoint algorithm and ORB-SURF algorithm have better stability under the condition of scale transformation. As shown in Fig. 12(d), under the condition of rotation transformation, the stability of the FLANN algorithm is poor, and the matching accuracy rate is obviously reduced. As shown in Fig. 12(e), the SuperPoint algorithm can effectively face the influence of rotation transformation. As shown in Fig. 12(f), the algorithm in this paper filters the edge-based feature points, eliminates some false matches, and improves the robustness of the matching algorithm. In Fig. 12 (g), Fig. 12 (h) and Fig. 12 (i), a matching experiment in which scale transformation and rotation transformation occur simultaneously is performed. The matching accuracy of ORB-SURF algorithm is much
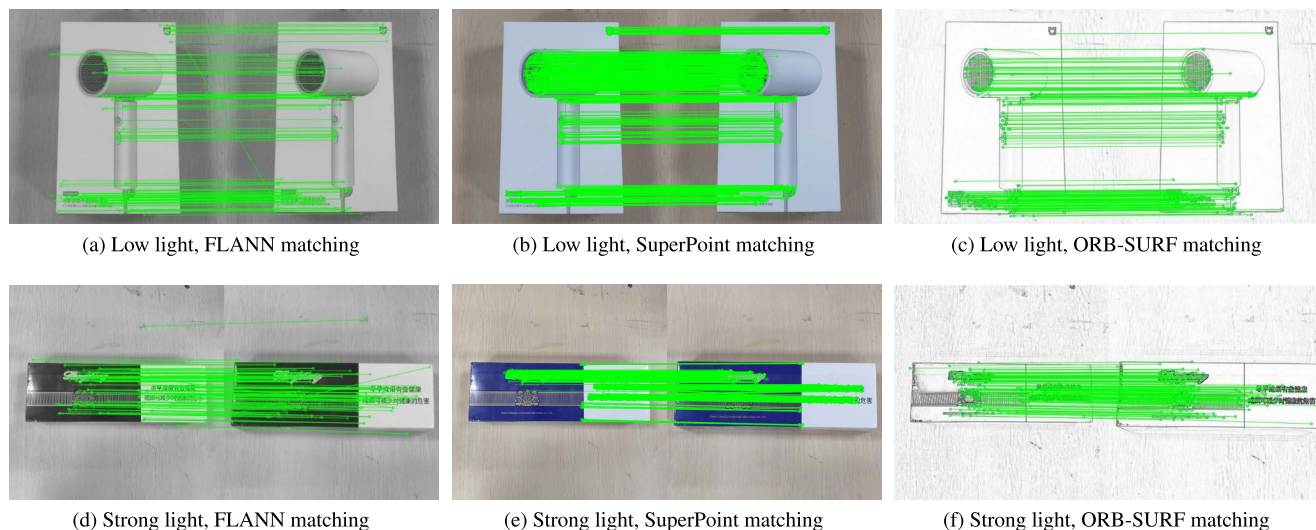
(a) Low light, FLANN matching   (b) Low light, SuperPoint matching   (c) Low light, ORB-SURF matching

(d) Strong light, FLANN matching   (e) Strong light, SuperPoint matching   (f) Strong light, ORB-SURF matching

FIGURE 11. Comparison experiment of light robustness.

(a) Scale transformation, FLANN matching   (b) Scale transformation, SuperPoint matching   (c) Scale transformation, ORB-SURF matching

(d) Rotation transformation, FLANN matching   (e) Rotation transformation, SuperPoint matching   (f) Rotation transformation, ORB-SURF matching

(g) Scale and Rotation transformation, FLANN matching   (h) Scale and Rotation transformation, SuperPoint matching   (i) Scale and Rotation transformation, ORB-SURF matching
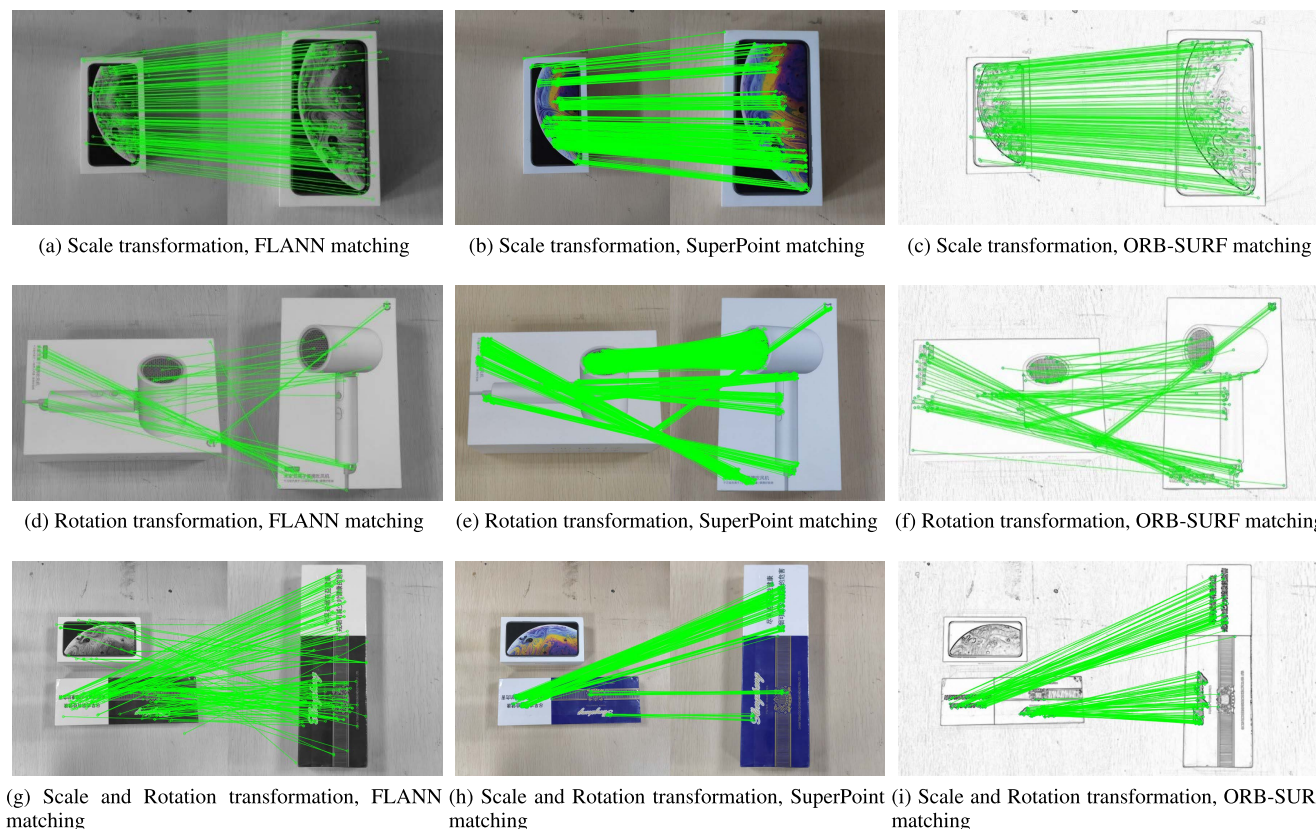
FIGURE 12. Robustness comparison experiment of scale transformation and rotation transformation.

higher than that of FLANN algorithm, but slightly lower than that of SuperPoint algorithm.

Table 4 shows the average response time and accuracy obtained by multiple sets of experiments under scale transformation and rotation transformation. In the case of scale transformation, the matching time of this algorithm is 27.73% lower than that of FLANN algorithm and 82.39% lower than that of SuperPoint algorithm. In the case of rotation transformation, the matching time of this algorithm is 30.32% lower than that of FLANN algorithm and 81.75% lower than that of SuperPoint algorithm. In the case of scale and rotation transformation, the matching time of this algorithm

TABLE 4. Robustness experimental results.

Experimental Conditions	Agorithm	Match Time /s	Matching Accuracy /%
	FLANN	1.738	92.26
Rotation Transformation	SuperPoint	7.132	99.37
	ORB-SURF	1.256	99.13
	FLANN	1.827	90.73
Scale Transformation	SuperPoint	6.976	99.20
	ORB-SURF	1.273	99.07
	FLANN	2.027	82.32
Scale and Rotation Transformation	SuperPoint	7.538	98.74
	ORB-SURF	1.316	98.37

is 35.08% lower than that of FLANN algorithm and 82.54% lower than that of SuperPoint algorithm. In terms of matching accuracy, the algorithm in this paper is slightly lower than SuperPoint algorithm, but it is significantly improved for FLANN algorithm. Therefore, the algorithm in this paper can effectively improve the correct rate of image matching in complex environments under the condition of ensuring a certain matching time.

VIII. CONCLUSION

Traditional matching methods have low matching accuracy, time-consuming matching, and are easily affected by scenes such as illumination transformation. By combining Sobel edge detection, an improved ORB-SURF algorithm is proposed in this paper. The algorithm improves on image edge feature, feature point extraction method, feature descriptor construction and feature point matching. Experimental results show that the improved algorithm has high matching accuracy in illumination, scale and rotation transformation scenes, with an average of 98.86%. The improved algorithm has greatly improved the matching speed, which is about 25% lower than the original SURF algorithm and about 80% lower than the SuperPoint algorithm. The improved algorithm further improves the problems of long time-consuming and low matching accuracy of the traditional algorithm. The improved algorithm eliminates the influence of lighting transformation scene on matching, and realizes adaptive matching. However, due to the long matching time of the ORB-SURF algorithm, it cannot better adapt to the real-time performance of closed-loop detection in visual SLAM. Therefore, the follow-up research work should further optimize the algorithm to improve the real-time performance of the algorithm.

REFERENCES

[1] J. Tang, "The application of computer vision in the medical field," *Commun. World*, vol. 26, no. 4, pp. 120–121, Apr. 2019.

[2] B. Li, S. Mao, and M. Li, "A robust method for dynamic image stitching on a fully mechanized mining face," *J. Geophys. Eng.*, vol. 18, no. 4, pp. 446–462, Jul. 2021, doi: 10.1093/jge/gxab023.

[3] L. Xuejie, Y. Xin, K. Hui, K. Heng, and Y. Chaoyu, "An image registration method based on improved TLD and improved ORB for mobile augmented reality," in *Proc. IEEE Int. Conf. Syst., Man, Cybern. (SMC)*, Oct. 2021, pp. 2127–2132.

[4] Z. Hossein-Nejad, H. Agahi, and A. Mahmoodzadeh, "Image matching based on the adaptive redundant keypoint elimination method in the SIFT algorithm," *Pattern Anal. Appl.*, vol. 24, no. 2, pp. 669–683, May 2021, doi: 10.1007/s10044-020-00938-w.

[5] X. Jiang, J. Ma, G. Xiao, Z. Shao, and X. Guo, "A review of multi-modal image matching: Methods and applications," *Inf. Fusion*, vol. 73, pp. 22–71, Sep. 2021.

[6] Z. Zhang, L. Wang, W. Zheng, L. Yin, R. Hu, and B. Yang, "Endoscope image mosaic based on pyramid ORB," *Biomed. Signal Process. Control*, vol. 71, Jun. 2021, Art. no. 103261.

[7] H. P. Morevec, "Techniques towards automatic visual obstacle avoidance," in *Proc. Int. Joint Conf. Artif. Intell.*, Feb. 1977, p. 584.

[8] C. Harris and M. Stephens, "A combined corner and edge detector," in *Proc. Alvey Vis. Conf.*, Aug. 1988, vol. 15, no. 50, pp. 5210–5244, doi: 10.1023/A:1008045108935.

[9] T. Lindeberg, "Feature detection with automatic scale selection," *Int. J. Comput. Vis.*, vol. 30, no. 2, pp. 77–116, 1998, doi: 10.1023/A:1008045108935.

[10] D. G. Lowe, "Distinctive image features from scale-invariant key-points," *Int. J. Comput. Vis.*, vol. 60, no. 2, pp. 91–110, 2004, doi: 10.1023/B:VISI.0000029664.99615.94.

[11] H. Bay, T. Tuytelaars, and L. Van Gool, "SURF: Speeded up robust features," *Comput. Vis. Image Understand.*, vol. 110, no. 3, pp. 404–417, Nov. 2006, doi: 10.1007/11744023_32.

[12] J.-Q. Song and X.-Y. Wang, "An improved SIFT matching algorithm based on Canny operator and K-L transform," *Telev. Technol.*, vol. 38, no. 15, p. 5, Aug. 2014.

[13] W. Chen, L. Yu, W. Yawei, S. Jing, J. Ting, and Z. Qinglin, "Fast image mosaic algorithm based on improved fast-surf," *J. Appl. Opt.*, vol. 42, no. 4, pp. 636–642, Jul. 2021.

[14] Z.-W. Wang, "Comparative study on the performance of several edge detection operators," *Manuf. Autom.*, vol. 34, no. 11, pp. 14–16, Jun. 2012.

[15] L. Li, S. Wang, W. Zeng, and F. Qin, "Research on zero watermarking technique based on improved Sobel operator," in *Proc. IEEE Int. Conf. Artif. Intell. Ind. Design (AIID)*, May 2021, pp. 594–597.

[16] R. Tian, G. Sun, X. Liu, and B. Zheng, "Sobel edge detection based on weighted nuclear norm minimization image denoising," *Electronics*, vol. 10, no. 6, p. 655, Mar. 2021, doi: 10.3390/electronics10060655.

[17] D.-Y. Li, "Optimal design of image edge detection based on Soble opera-tor," *Digit. Technol. Appl.*, vol. 11, pp. 137–138, Nov. 2017.

[18] C.-G. Miao and C. Liu, "Gray image edge detection based on improved Sobel operator," *Internet Things Technol.*, vol. 10, no. 11, pp. 37–38 and 41, Nov. 2020.

[19] G. Ravivarma, K. Gavaskar, D. Malathi, K. G. Asha, B. Ashok, and S. Aarthi, "Implementation of Sobel operator based image edge detection on FPGA," *Mater. Today, Proc.*, vol. 45, pp. 2401–2571, May 2021, doi: 10.1016/j.matpr.2020.10.825.

[20] E. Rublee, V. Rabaud, K. Konolige, and G. Bradski, "ORB: An efficient alternative to SIFT or SURF," in *Proc. Int. Conf. Comput. Vis.*, Jan. 2011, pp. 2564–2571.

[21] E. Rosten and T. Drummond, "Fusing points and lines for high perfor-mance tracking," in *Proc. 10th IEEE Int. Conf. Comput. Vis. (ICCV)*, Oct. 2005, pp. 1508–1515.

[22] S. Li, "Research on SLAM loop detection based on ORB feature matching algorithm," M.S. thesis, Softw. Eng., Beijing Univ. Technol., Beijing, China, 2020.

[23] M. Gupta and P. Singh, "An image forensic technique based on SIFT descriptors and FLANN based matching," in *Proc. 12th Int. Conf. Comput. Commun. Netw. Technol. (ICCCNT)*, Jul. 2021, pp. 1–7.

[24] M. Muja and D. Lowe, "FLANN—Fast library for approximate nearest neighbors user manual," Dept. Comput. Sci., May 2009, vol. 3, pp. 1–22.

[25] J.-F. Luo et al., ''Research on surf binocular vision matching algorithm based on adaptive double threshold,'' *J. Instrum.*, vol. 41, no. 3, pp. 240–247, Mar. 2020.

[26] D. DeTone, T. Malisiewicz, and A. Rabinovich, ''SuperPoint: Self-supervised interest point detection and description,'' in *Proc. IEEE/CVF Conf. Comput. Vis. Pattern Recognit. Workshops (CVPRW)*, Jun. 2018, pp. 224–236.

YI ZHANG received the Ph.D. degree from the Huazhong University of Science and Technology (HUST), Wuhan, China. He is currently a Professor with the School of Advanced Manufacturing Engineering, Chongqing University of Posts and Telecommunications (CQUPT). His research interests include intelligent systems and mobile robots and intelligent logistics technology and equipment.

LENG HAN received the M.S. degree from the Chongqing University of Posts and Telecommunications (CQUPT), Chongqing, China. He is currently a Senior Engineer with the Chongqing University of Posts and Telecommunications. His research interests include algorithm research and digital signal processing.

XIA SUN received the M.S. degree from the Chongqing University of Posts and Telecommunications (CQUPT), Chongqing, China. She is currently an Associate Professor with the Chongqing Institute of Engineering. Her research interests include wireless mobile communication technology, algorithm research, and digital signal processing.

JIAWEI WANG received the B.S. degree from the Chongqing University of Science and Technology (CQUST), Chongqing, China, in 2020. He is currently pursuing the master's degree with the School of Advanced Manufacturing Engineering, Chongqing University of Posts and Telecommunications (CQUPT). His current research interests include mobile robot and V-SLAM.

XUHUI WU received the B.S. degree from Lanzhou Jiaotong University (LZJTU), Lanzhou, China, in 2017. He is currently pursuing the master's degree with the School of Advanced Manufacturing Engineering, Chongqing University of Posts and Telecommunications (CQUPT). His current research interests include mobile robot and laser SLAM.

· · ·